AMERICAN SOCIETY FOR MICROBIOLOGY | Infection and Immunity®

HOST RESPONSE AND INFLAMMATION

In Vivo Imaging of the Buccal Mucosa Shows Loss of the Endothelial Glycocalyx and Perivascular Hemorrhages in Pediatric *Plasmodium falciparum* Malaria

Eric Lyimo,[a] Lars Emil Haslund,[b] Thomas Ramsing,[b] Christian William Wang,[c,d] Akinwale Michael Efunshile,[e] Alphaxard Manjurano,[a] Victor Makene,[f] John Lusingu,[g] Thor Grundtvig Theander,[c,d] Jørgen Anders Lindholm Kurtzhals,[c,h] Rasmus Paulsen,[b] Casper Hempel[i]

[a]National Institute for Medical Research (NIMR), Mwanza, Tanzania
[b]Department for Computer Sciences, Technical University of Denmark, Kongens Lyngby, Denmark
[c]Centre for Medical Parasitology, Department for Immunology and Microbiology, University of Copenhagen, Copenhagen, Denmark
[d]Department of Infectious Diseases, Copenhagen University Hospital (Rigshospitalet), Copenhagen, Denmark
[e]Department of Medical Microbiology, Federal Teaching Hospital/Ebonyi State University, Abakaliki, Nigeria
[f]University of Dar es Salaam, Dar es Salaam, Tanzania
[g]National Institute for Medical Research (NIMR), Tanga, Tanzania
[h]Department of Clinical Microbiology, Copenhagen University Hospital, Copenhagen, Denmark
[i]Department of Health Technology, Technical University of Denmark, Kongens Lyngby, Denmark

ABSTRACT Severe malaria is mostly caused by *Plasmodium falciparum,* resulting in considerable, systemic inflammation and pronounced endothelial activation. The endothelium forms an interface between blood and tissue, and vasculopathy has previously been linked with malaria severity. We studied the extent to which the endothelial glycocalyx that normally maintains endothelial function is involved in falciparum malaria pathogenesis by using incident dark-field imaging in the buccal mucosa. This enabled calculation of the perfused boundary region, which indicates to what extent erythrocytes can permeate the endothelial glycocalyx. The perfused boundary region was significantly increased in severe malaria patients and mirrored by an increase of soluble glycocalyx components in plasma. This is suggestive of a substantial endothelial glycocalyx loss. Patients with severe malaria had significantly higher plasma levels of sulfated glycosaminoglycans than patients with uncomplicated malaria, whereas other measured glycocalyx markers were raised to a comparable extent in both groups. In severe malaria, the plasma level of the glycosaminoglycan hyaluronic acid was positively correlated with the perfused boundary region in the buccal cavity. Plasma hyaluronic acid and heparan sulfate were particularly high in severe malaria patients with a low Blantyre coma score, suggesting involvement in its pathogenesis. *In vivo* imaging also detected perivascular hemorrhages and sequestering late-stage parasites. In line with this, plasma angiopoietin-1 was decreased while angiopoietin-2 was increased, suggesting vascular instability. The density of hemorrhages correlated negatively with plasma levels of angiopoietin-1. Our findings indicate that as with experimental malaria, the loss of endothelial glycocalyx is associated with vascular dysfunction in human malaria and is related to severity.

KEYWORDS endothelial glycocalyx, microcirculation, malaria, incident dark-field imaging, image analyses, *Plasmodium falciparum*, glycocalyx shedding

Severe malaria (SM) is caused by *Plasmodium falciparum*, a parasite that invades and multiplies in human erythrocytes. The pathogenesis of SM involves the cytoadhesion of parasitized erythrocytes, leading to impaired blood flow and dysregulated

Citation Lyimo E, Haslund LE, Ramsing T, Wang CW, Efunshile AM, Manjurano A, Makene V, Lusingu J, Theander TG, Kurtzhals JAL, Paulsen R, Hempel C. 2020. *In vivo* imaging of the buccal mucosa shows loss of the endothelial glycocalyx and perivascular hemorrhages in pediatric *Plasmodium falciparum* malaria. Infect Immun 88:e00679-19. https://doi.org/10.1128/IAI.00679-19.

Editor Jeroen P. J. Saeij, UC Davis School of Veterinary Medicine

Address correspondence to Casper Hempel, casperhempel@gmail.com.

Received 27 August 2019
Returned for modification 16 September 2019
Accepted 16 December 2019
Accepted manuscript posted online 23 December 2019
Published 20 February 2020

TABLE 1 Baseline characteristics of patients from the Tanzanian cohort[a]

Characteristic	Value for:			
	Healthy subjects ($n = 31$)	NMF patients ($n = 7$)	UM patients ($n = 12$)	SM patients ($n = 69$)
Age (yrs)	2.6 (0.8–4.3)	2.28 (1.0–4.0)	5.5 (1.1–10.1)	4.1 (0.6–10.0)
Sex (% females)	21	67	62	48
Parasitemia (no./μl blood)	0	0	55,560 (1,360–156,560)	53,560 (1,000–2,789,320)
Hemoglobin (g/dl)	8.5 (6.2–11.3)	6.8 (2.2–11.3)	9.3 (7.0–13.4)	7.4 (2.3–12.6)
Glucose (mmol/liter)	ND	7.8 (6.9–9.2)	6.2 (3.8–8.2)	6.8 (1.4–26.6)
Lactate (mmol/liter)	ND	5.5 (4.6–7.4)	4.1 (3.1–5.0)	7.4 (2.4–21.9)

[a]Subjects were stratified into category of disease. ND, not determined. Most data are presented as means and ranges; parasitemia values are presented as medians and ranges. NMF, nonmalaria fever; UM, uncomplicated malaria; SM, severe malaria.

coagulation and inflammation (1). The inflammatory state causes remodeling of the endothelial surface, including upregulation of immune receptors on the vasculature (2–4) and further interactions between the vasculature and malaria-infected erythrocytes and leukocytes (5, 6). The severity of malaria depends partly on what variant surface antigens the parasites express and export to the erythrocyte surface (7, 8). Also, endothelial responsiveness to inflammatory cytokines contributes to determining whether an infection results in SM or uncomplicated malaria (UM) (9). Plasma markers of endothelial activation correlate strongly with malaria severity and discriminate between SM and UM, suggesting that the level of vasculopathy is a strong predictor for the outcome of *P. falciparum* malaria (3, 10).

One part of the endothelium that responds to activation and inflammation is the dense matrix of carbohydrates termed the endothelial glycocalyx (11). The endothelial glycocalyx covers the luminal surface of healthy blood vessels and plays several roles in maintaining vascular homeostasis: it shields immune receptors from unwanted binding, it is a mechanosensor, and it is involved in reducing permeability over the vasculature (5, 12–14). The endothelial glycocalyx is shed in response to inflammatory conditions and has been studied in several diseases, including diabetes (15) and sepsis (16), and in viral infections (17, 18).

In experimental murine malaria, we have previously shown an association between malaria severity and glycocalyx loss in brain vessels (19, 20). Murine malaria models have been debated (21), and we were thus interested in addressing whether the loss of endothelial glycocalyx is involved in the pathogenesis of human *P. falciparum* malaria. If so, one would expect an association between the extent of glycocalyx loss and the severity of *P. falciparum* malaria. It has recently been shown that plasma levels of the glycosaminoglycan chondroitin sulfate and the proteoglycan syndecan-1 are increased in adult, Asian malaria patients and the latter marker also in the plasma of Ugandan children (22–24). Levels of chondroitin sulfate in urine have also been shown to increase in SM. Here, we provide detailed analysis of the glycocalyx loss associated with pediatric *P. falciparum* malaria and its association with impaired microcirculation, using state-of-the-art noninvasive imaging of the buccal mucosa.

RESULTS

Patients. The children enrolled are described in Table 1. The ages, 0 to 10 years, varied between the four groups ($P = 0.02$), and *post hoc* tests showed that UM patients were significantly older than healthy children and patients with nonmalaria fever (NMF) ($P = 0.01$ and $P = 0.047$, respectively). Gender distributions were marginally different between the four groups ($P = 0.047$). Parasitemia and plasma glucose levels were similar in UM and SM patients ($P = 0.4$ and $P = 0.2$, respectively). SM patients had significantly lower levels of plasma hemoglobin (Hb) and higher levels of lactate than UM patients ($P < 0.01$). None of the admitted patients died from the infection. Eight patients had temporarily decreased consciousness after a seizure, but these did not formally meet the criteria for cerebral malaria. The distribution of criteria defining SM is summarized in Table 2.

IDF imaging shows perivascular hemorrhages and sequestration in the buccal microcirculation. Incident dark-field (IDF) imaging was used to visualize erythrocyte

TABLE 2 Breakdown of the SM subgroup[a]

Characteristic	No. of SM patients with characteristic
Plasma lactate level of >5 mmol/liter	56
Hyperparasitemia	24
Severe anemia	14
Seizures	8
BCS ≤ 2	8

[a]Patients were enrolled in the SM group due to hyperparasitemia, severe anemia, or a Blantyre coma score (BCS) of ≤2. Some patients belonged to more than one of the subgroups.

movements in the buccal microcirculation. Healthy subjects had strictly delineated blood vessels, as shown in a representative still image (Fig. 1A). The vascular integrity in the buccal cavity was frequently impaired in malaria patients, showing stagnant erythrocytes outside blood vessels (Fig. 1B and C). Perivascular hemorrhages were common in SM patients but not in controls; approximately 50% of all SM patients had some degree of perivascular hemorrhaging. The proportions of subjects with perivascular hemorrhages were significantly different when all groups were compared ($P = 0.04$), although the difference between SM and UM patients did not reach significance in *post hoc* tests ($P = 0.15$). The densities of perivascular hemorrhages were comparable between the groups (Fig. 1D) (SM versus healthy controls, $P = 0.09$).

IDF imaging furthermore showed late-stage parasites sequestering in the microvessels (Fig. 1E; see Movie S1 in the supplemental material). *In vitro* studies allowed us to substantiate that the dark cells clearly marked by well-defined edges present in and around microvessels are late-stage parasites (Fig. S2). Thus, the Prewitt filter allows for unbiased detection of late-stage parasites (Fig. S3 and Movie S2).

IDF imaging shows loss of endothelial glycocalyx. Image analyses of the microvessels enabled detection of spatiotemporal movements of erythrocytes. The median diameter of blood vessels analyzed was 23.1 μm, which is in the range of postcapillary venules, and this diameter was similar for all groups ($P = 0.8$). An example of three temporally separated segments is shown in Fig. 2A, and from the full stack of images, the corresponding diameters for the median and minimum filters are calculated and shown (Fig. 2B). Calculating the diameter at the same localization for both filters allowed us to calculate the perfused boundary region (PBR) (Fig. 2C). The PBR measures how well erythrocytes penetrate the glycocalyx (25). Since there is an inverse relationship between PBR and the thickness of the glycocalyx, a high PBR indicates a thin glycocalyx. The median PBR was significantly increased in SM patients in comparison with that in healthy children ($P < 0.0001$) (Fig. 2D). The median PBRs of UM and SM patients were comparable. Since an increased PBR could be associated with clinical features, as seen in experimental models (20), we tested if SM patients with a Blantyre coma score (BCS) of less than 3 ($n = 5$; median PBR, 4.5 μm) had higher PBRs than SM patients with a higher BCS ($n = 38$; median PBR, 3.9 μm) and found a nonsignificant trend ($P = 0.09$).

The proportions of perfused vessels (PPV) were similar in all groups ($P = 0.2$) (Fig. S4A). The average flow speed differed significantly between groups ($P = 0.03$) (Fig. S4B). This could be explained by the anemia, since SM patients with anemia had a significantly higher average speed of blood flow than healthy children ($P = 0.006$) and since flow speed was negatively correlated with plasma Hb (rho = -0.2, $P = 0.04$). Despite focal hypoperfusion, the heterogeneity indexes were similar in malaria patients and healthy children ($P > 0.9$) (Fig. S4C) but significantly increased in NMF patients ($P = 0.03$).

Increased plasma levels of glycocalyx components in malaria patients. An increased PBR implies that the glycocalyx is perturbed and possibly shed in the circulation in malaria patients. In concordance with this, plasma hyaluronic acid (HA) and sulfated glycosaminoglycan (GAG) levels were significantly increased in SM patients (Fig. 3A and B) ($P < 0.001$), with *post hoc* analysis showing significance for SM patients compared with healthy controls ($P < 0.01$). UM and SM patients as well as SM

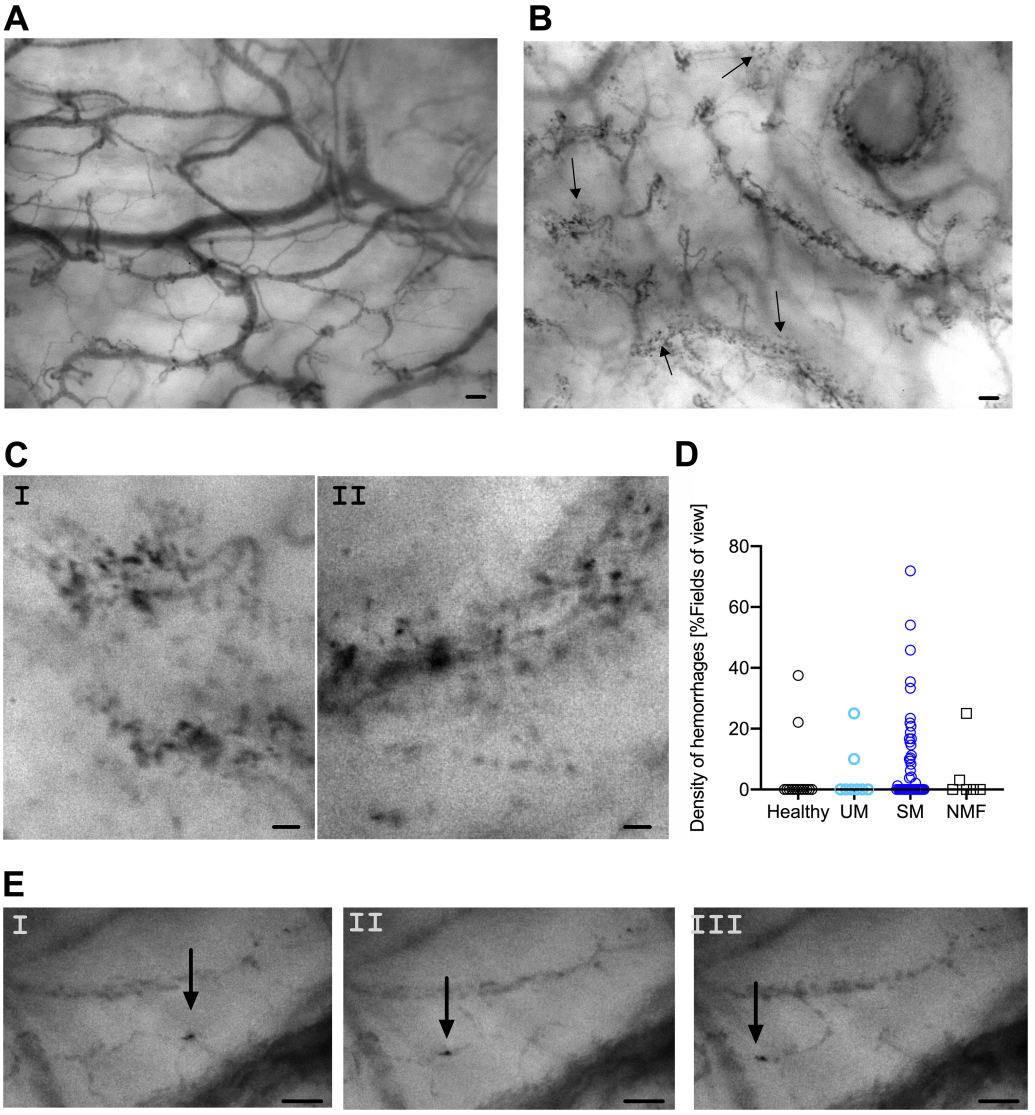

FIG 1 IDF imaging shows malaria-induced changes in the buccal microcirculation. (A) A still image of a healthy volunteer showing highly delineated blood vessels. (B) A still image from malaria-infected individuals with multiple hemorrhages. (A still image of a malaria-infected individual without hemorrhage is seen in Fig. S1 in the supplemental material.) Arrows in panel B denote perivascular hemorrhages. (C) Close-ups of representative hemorrhages; panel I is selected from the still shown in panel B, while panel II is a close-up from a different still image. (D) Density of perivascular hemorrhages as determined by IDF imaging. (E) Still images from a movie showing an infected erythrocyte sequestering in a capillary (Movie S1). Still images are temporally separated by 40 ms. Scale bars, 100 μm (A and B) and 50 μm (C and E).

and NMF patients were not significantly different in terms of HA, whereas levels of sulfated GAGs were significantly higher in SM than in UM patients ($P = 0.02$). Plasma levels of heparan sulfate (HS) and syndecan-1 were significantly increased in SM patients (Fig. 3C and D) ($P < 0.0001$), and for HS, a significant increase was also seen in UM patients ($P = 0.003$). Plasma levels of HS and syndecan-1 were comparable between UM and SM patients ($P > 0.9$), and these groups had levels of shed HS that were comparable with those of NMF patients ($P > 0.4$). NMF, which did not affect PBR, did not change the levels of these plasma components ($P > 0.2$). Plasma levels of syndecan-4 were not changed in any of the groups ($P = 0.7$), whereas glypican-1 was significantly increased in SM and NMF patients (Fig. 3E) ($P = 0.02$ for both groups). Glypican-1 levels were comparable between SM and UM patients ($P > 0.9$). The HA receptor CD44 did not vary between groups ($P = 0.8$).

The visually detected glycocalyx loss in the buccal mucosa of SM patients showed an association with plasma levels of HA (Fig. 4A) (rho = 0.7, $P < 0.0001$) but not with

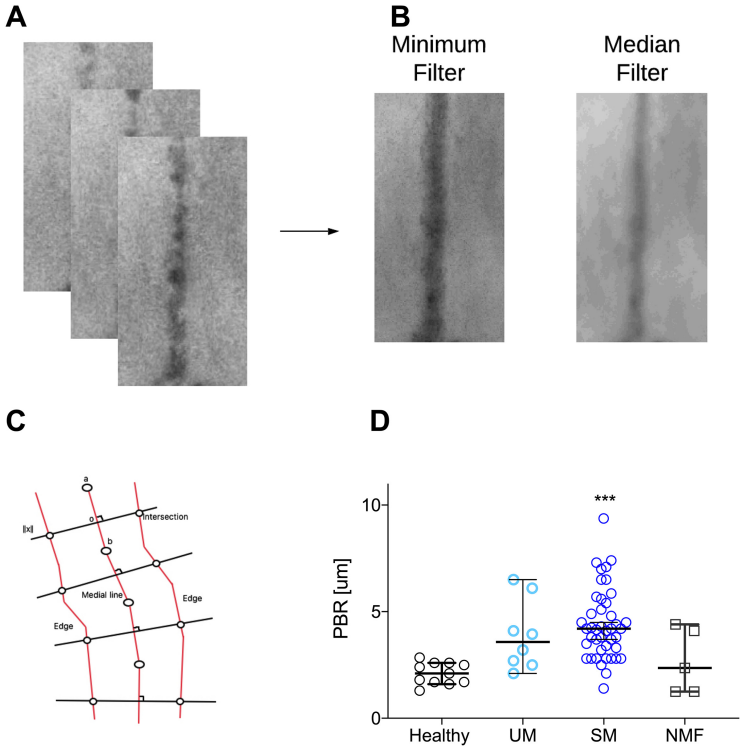

FIG 2 Quantitative analyses of IDF imaging show substantial loss of endothelial glycocalyx in the buccal cavity as measured by increased PBR. (A) A temporal sequence of vessel segments. (B) The corresponding minimum and median filters. (C) Model of measurement of the Euclidian distance. The shortest path is calculated (centered line) and perpendicular to this, the Euclidian distance is calculated after application of a minimum and a medium filter. (D) The PBR was significantly increased in SM ($P < 0.0001$) as well as in UM ($P = 0.04$) patients compared to healthy controls. All data points represent one individual. Data are summarized as medians (for average speed, the mean is shown), and error bars show 95% confidence intervals. ***, *P* value of <0.001; **, *P* value of <0.01 and >0.001; *, *P* value of <0.05 and >0.01.

other glycocalyx components. Because there was a trend toward a higher PBR in SM patients with a low BCS, we tested if this was reflected in any of the plasma markers of glycocalyx shedding. Both plasma HA and HS levels were significantly increased in SM patients with a low BCS in comparison with those in SM patients with a higher BCS (Fig. 4B and C) ($P = 0.01$ and $P = 0.005$, respectively). Plasma levels of glycocalyx components were correlated with neither parasite counts nor with the density of hemorrhages in the buccal mucosa (data not shown). It could be speculated that glycocalyx loss was secondary to anaerobic metabolism, induced by impaired microcirculation, but glycocalyx markers did not correlate with plasma lactate levels ($P > 0.16$).

Shedding of endothelial glycocalyx components correlates with markers of endothelial activation. Plasma angiopoietin-1 decreased significantly in SM patients (Fig. 5A) ($P < 0.0001$) with *post hoc* tests showing significance for SM but not UM and NMF patients. Plasma levels of angiopoietin-2 were significantly increased in SM patients (Fig. 5B) and ($P < 0.0001$) but not in NMF or UM patients ($P > 0.4$). Levels of the vasoconstrictor endothelin-1 increased significantly in SM and UM patients (Fig. 5C) ($P = 0.002$ and $P = 0.02$, respectively). Finally, the levels of soluble thrombomodulin, which is involved in both coagulation and inflammation, increased in SM patients compared with healthy controls and NMF (Fig. 5D) ($P = 0.002$ and $P = 0.04$, respectively).

In SM patients, plasma angiopoietin-1 was negatively associated with HA levels (rho = −0.31, $P = 0.02$) and with density of hemorrhages (Fig. 5E) (rho = −0.36, $P = 0.02$) but not with angiopoietin-2 ($P = 0.9$). All subjects with hemorrhages in the buccal cavity had plasma angiopoietin-1 levels below 20 ng/ml. Angiopoietin-2 was positively associated with syndecan-1 (rho = 0.5, $P = 0.001$) and with HS levels

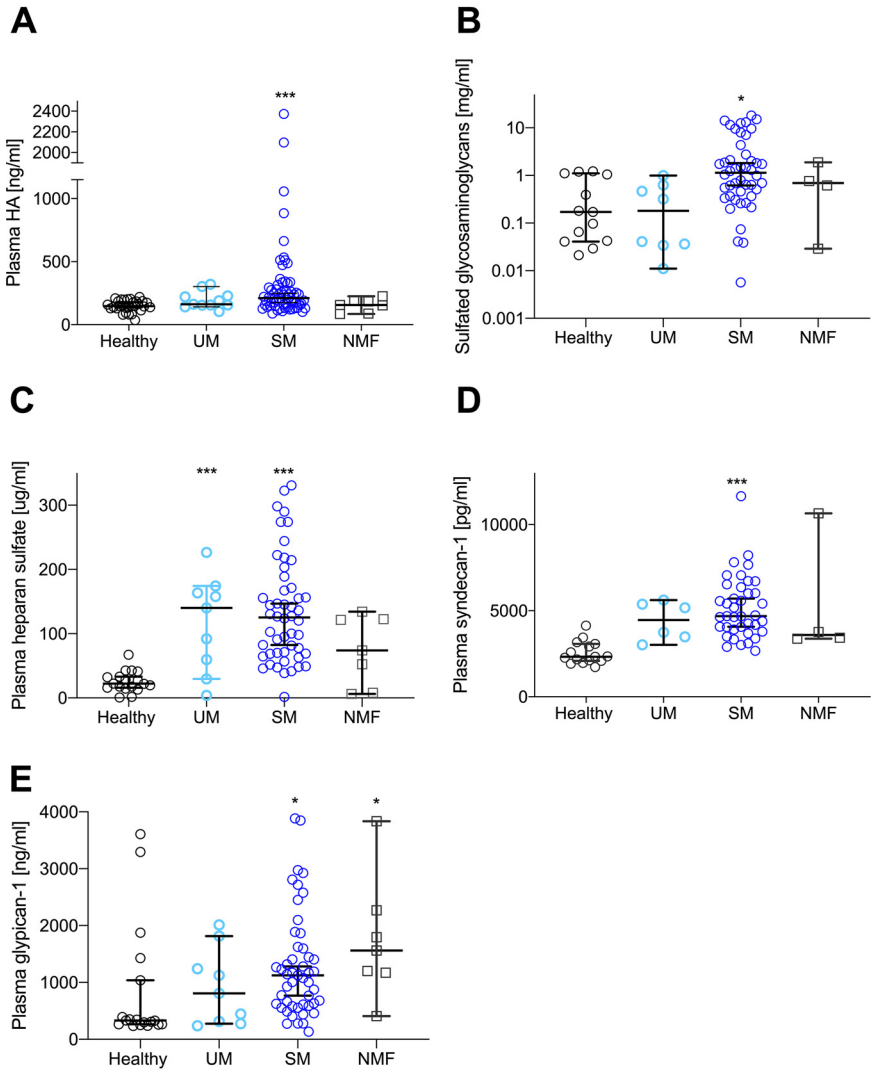

FIG 3 Glycocalyx components are shed and detected at an increased level in the plasma of patients with SM. (A) Plasma HA increased significantly in SM patients ($P < 0.0005$) but not in patients with UM. (B) Sulfated GAGs in plasma increased significantly in patients with SM ($P = 0.01$) compared with healthy controls, and levels in SM patients were increased compared with those in UM patients ($P = 0.02$). (C) Plasma HS increased significantly in SM patients ($P < 0.0001$) and also in UM patients ($P = 0.003$). Plasma levels of HS were comparable in UM and SM patients. (D) Compared with that in healthy subjects, plasma syndecan-1 increased significantly in SM patients ($P < 0.0001$). Plasma levels of syndecan-1 were comparable in UM and SM patients. (E) Glypican-1 increased significantly in SM ($P = 0.02$) and NMF ($P = 0.02$) patients. Plasma levels of glypican-1 were comparable in UM and SM patients. All data points represent one individual. Data are summarized as medians, and error bars show 95% confidence intervals. ***, *P* value of <0.001; **, *P* value of <0.01 and >0.001; *, *P* value of <0.05 and >0.01.

(rho = 0.34, $P = 0.03$). Also, thrombomodulin was positively associated with PBR (Fig. 5F) (rho = 0.38, $P = 0.02$).

Plasma levels of the proinflammatory cytokine tumor necrosis factor (TNF) and plasma E-selectin were significantly increased in SM patients ($P < 0.0001$ versus healthy controls for both markers) (Fig. S5A and B).

Glycocalyx components are cleared slowly from the plasma. Five SM and four UM patients returned for follow-up investigations. IDF imaging showed that microhemorrhages persisted to some extent as long as 28 days after admission. The gradual reduction of hemorrhages appeared faster in UM than in SM patients, but the low number of follow-up patients precludes any meaningful comparison between the groups. PBR and HA and syndecan-1 levels returned to those of healthy controls at day

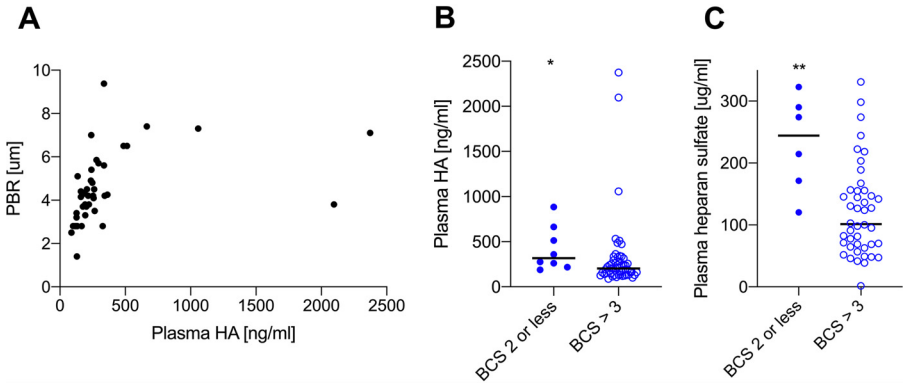

FIG 4 Some glycocalyx components in the plasma are particularly high in patients with a low BCS. (A) Plasma HA correlated positively with PBR ($P < 0.0001$). (B) Plasma HA was significantly increased in plasma from SM individuals with a low BCS compared with patients without ($P = 0.01$). (C) Plasma HS was significantly increased in plasma from SM individuals with a low BCS compared with patients without ($P = 0.005$). All data points represent one individual. Data are summarized as medians, and error bars show 95% confidence intervals. ***, *P* value of <0.001; **, *P* value of <0.01 and >0.001; *, *P* value of <0.05 and >0.01.

28 postadmission (Fig. 6A to C). In patients with UM and SM, HA levels stayed elevated at day 14 after admission, while being significantly reduced and comparable with those in healthy controls at day 28 (Fig. 6B) ($P = 0.03$). The persistent increase in shed glycocalyx components was to some extent mirrored by plasma angiopoietin-1 levels, but these were temporal changes that were not significant (Fig. 6D) ($P > 0.07$). Also, angiopoietin-2 levels seemed to drop but not significantly (Fig. 6E) ($P > 0.07$). These persistent signatures are mirrored by E-selectin levels that were also normalized (i.e., significantly lower than at day 0) at day 28 postadmission (Fig. 6F) ($P = 0.03$).

We hypothesized that the level of glycocalyx components in the plasma would correlate with the level of TNF over time, but this was not the case for any glycocalyx component ($P > 0.2$).

DISCUSSION

By using state-of-the-art *in vivo* imaging of the microcirculation, we were able to quantify the loss of the endothelial glycocalyx and identify other malaria-induced microcirculatory changes in the buccal microvessels. Increased numbers of microhemorrhages, thinning of the glycocalyx, and plasma levels of shed HS and HA were associated with disease severity. This indicates that the glycocalyx loss previously shown in experimental malaria (19, 20) also occurs in human *P. falciparum* malaria and may contribute to disease severity.

In vivo imaging using IDF allowed us to assess the microcirculation to unprecedented detail in real time. This enabled demonstration of microvascular alterations and showed *in vivo* evidence of malaria-infected erythrocytes sequestering in the microcirculation and frequent perivascular hemorrhages. The finding that the buccal microcirculation is impaired in malaria points toward a systemic intravascular accumulation of infected erythrocytes, as previously described (26). One previous study using *in vivo* imaging in adult malaria patients from Asia showed obstructed vessels and heterogeneous flow patterns in the rectal mucosal during cerebral malaria (CM) but to a less pronounced degree in the sublingual mucosa (27), suggesting notable regional differences in the microcirculation. There are clear differences between adult and pediatric SM, and microvascular damage and perivascular hemorrhages may be of particular importance in children (1).

IDF imaging can also indicate whether patients have loss of hemodynamic coherence as seen in, e.g., sepsis (28). We did not notice a change in the PPV or heterogeneity, suggesting that obstruction of microvessels in the buccal cavity was not pronounced. Another factor leading to loss of hemodynamic coherence is hemodilution

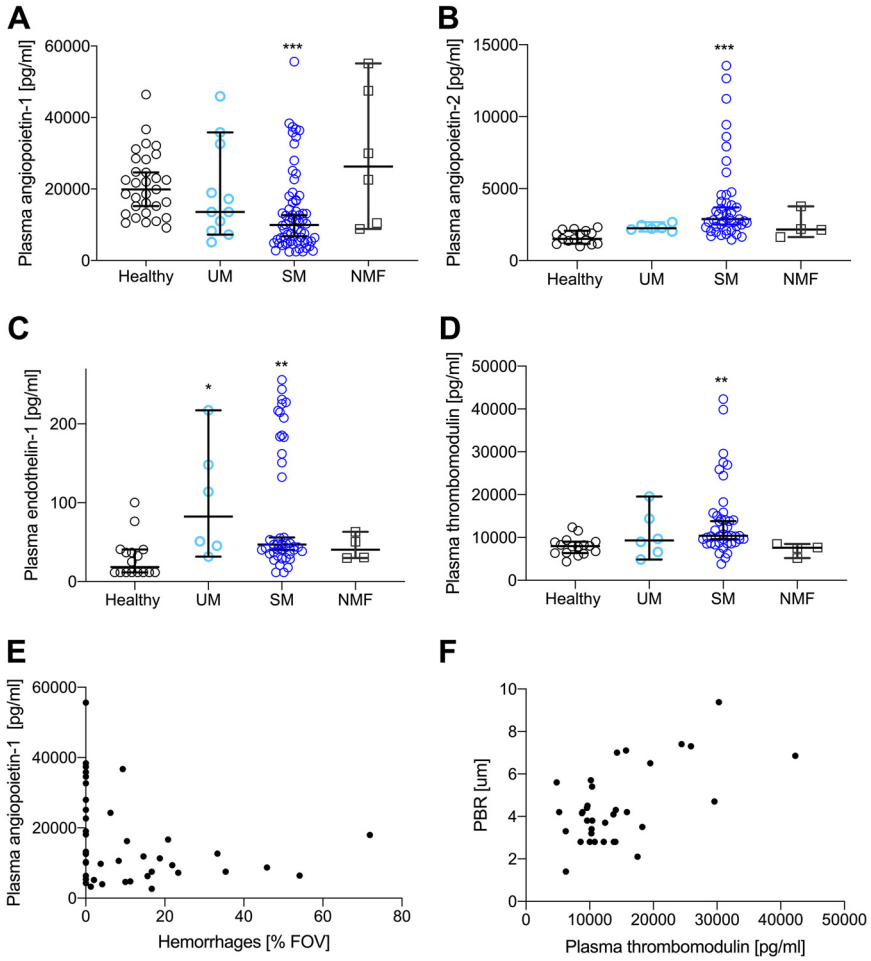

FIG 5 Plasma markers show marked endothelial dysfunction and associations with impaired microcirculation. (A) Plasma angiopoietin-1 decreased significantly in SM patients ($P = 0.0002$). No change was seen for UM and NMF patients. (B) Angiopoietin-2 levels increased significantly in SM patients ($P < 0.0001$). (C) Plasma endothelin-1 was increased in SM ($P = 0.002$) and UM ($P = 0.02$) patients. (D) Plasma thrombomodulin was significantly increased in SM patients ($P = 0.002$). Plasma levels for all four markers were comparable in UM and SM patients. (E). Plasma angiopoietin-1 correlated negatively with the frequency of hemorrhages detected in the fields of views analyzed (rho = −0.36, $P = 0.02$). (F) Plasma thrombomodulin was positively correlated with PBR (rho = 0.38, $P = 0.02$). All data points represent one individual. Data are summarized as medians, and error bars show 95% confidence intervals. ***, P value of <0.001; **, P value of <0.01 and >0.001, *, P value of <0.05 and >0.01.

(29). In SM patients with anemia, we saw significantly increased red blood cell (RBC) velocity, which was negatively correlated with Hb. It has been suggested that moderate anemia plays a protective role in patients with SM, possibly due to hemodilution leading to improved blood flow (30). Our IDF findings support this hypothesis.

IDF imaging showed that perivascular hemorrhages in the buccal mucosa were frequent in SM patients and differed in numbers between patients similarly to what is seen with retinal assessment during CM (31). The number of perivascular hemorrhages was negatively correlated with plasma angiopoietin-1, supporting the role of angiopoietin-1 in prevention of vascular leakage (32). Our data suggest that perivascular hemorrhages in SM are mostly seen when plasma angiopoietin-1 gets below 20 ng/ml. This drop corresponds with low angiopoietin-1 levels that have been associated with malaria severity in studies in African children (3, 4).

Our *in vitro* experiments showed late-stage infected erythrocytes appearing as dark spots with clearly defined edges. This can be explained by hemozoin absorbing light at 525 nm to a greater extent than Hb (33). Since the *in vitro* experiment was conducted in the absence of leukocytes, we cannot rule out the possibility that some of the

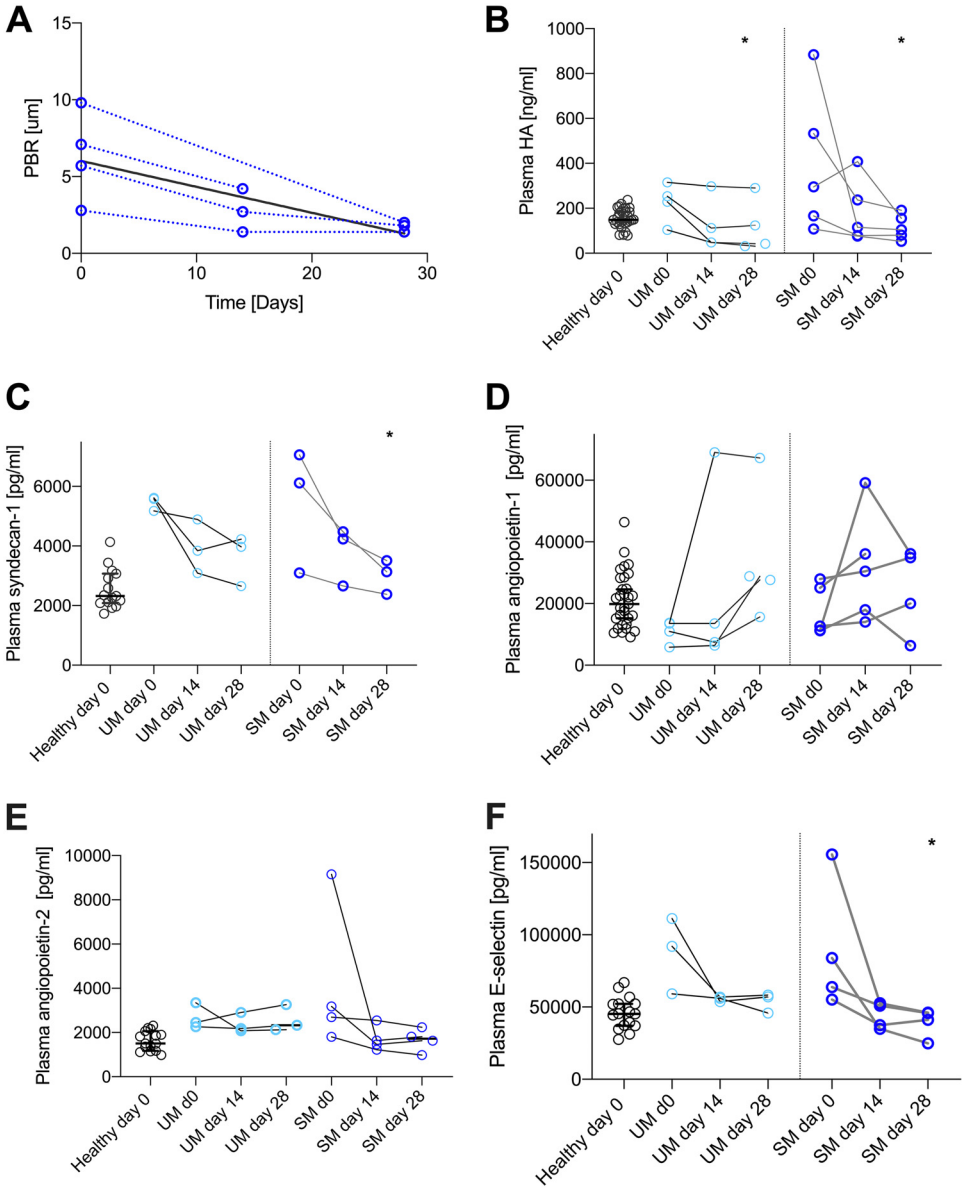

FIG 6 Glycocalyx components are increased in plasma for several weeks after admission. (A) PBR persisted to be increased but decreased to levels comparable to those of healthy controls at day 28 postadmission. The bold black line shows the linear regression of the data points. (B) Plasma HA decreased significantly at day 28 postadmission ($P = 0.02$), while no change in comparison to day 0 was noted at day 14 postadmission ($P = 0.4$). Also, in UM patients, a time-dependent decrease was seen ($P = 0.03$, day 0 versus day 28). (C) Plasma syndecan-1 levels were significantly reduced at day 28 in SM patients ($P = 0.03$). (D) Plasma angiopoietin-1 levels did not change significantly during 28 days postadmission. (E) Plasma levels of angiopoietin-2 decreased but not significantly in comparison with levels at admission. (F) Plasma E-selectin levels were reduced back to normal levels at day 28 postadmission ($P = 0.03$). All data points represent one individual. Data are summarized as medians, and error bars show 95% confidence intervals. ***, P value of <0.001; **, P value of <0.01 and >0.001; *, P value of <0.05 and >0.01.

perivascular spots that were observed in the buccal mucosa *in vivo* were hemozoin-containing leukocytes (34, 35).

A main purpose of using IDF imaging was to assess glycocalyx loss. We designed software to automatically calculate the PBR in random vessel segments in an unbiased manner. PBR has previously been used to assess glycocalyx loss in, e.g., obese patients (25). Our analysis showed significantly larger PBR in SM patients than in healthy controls, providing direct *in vivo* evidence for malaria-induced glycocalyx loss in humans. The use of PBR as an indicator of glycocalyx shedding was further supported

by the positive correlation between PBR and plasma HA. HA constitutes an outer flexible part of the glycocalyx acting as a canopy (36), which could explain why HA showed the strongest association with PBR of the glycocalyx components. The study we performed in a Nigerian cohort (see Fig. S5 in the supplemental material), as well as other studies, further supports the loss of the endothelial glycocalyx in *P. falciparum* malaria (22–24).

An increase in PBR during malaria implies that the infected erythrocytes can penetrate deeper into the glycocalyx, getting in close contact with receptors anchored on the endothelial surface. A healthy glycocalyx leaves only nanometer-sized pores open to entry (37), thereby shielding endothelial receptors (12, 38), and *in vitro* it prevents infected erythrocytes from optimally interacting with CD36 (39). SM patients with a low BCS had significantly higher plasma levels of some GAGs, suggesting that glycocalyx shedding is associated with disease severity.

Glycocalyx loss has been seen in other diseases involving inflammation and endothelial activation (15, 17, 18, 25) and is, thus, not unique to malaria. However, *P. falciparum* uses endothelial receptors for cytoadhesion, and changes to the glycocalyx may lead to increased exposure of, e.g., CD54, as previously shown *in vitro* (39).

Patients with impaired consciousness had signs of endothelial glycocalyx loss. In sepsis, it was recently shown that circulating HS components were associated with cognitive impairment, since they have affinity for brain-derived neurotrophic factor (40). Whether circulating HS fragments also contribute to cognitive impairment in cerebral malaria needs further investigation.

Finally, IDF imaging enabled us to assess the PBR over time, demonstrating that the restoration of the glycocalyx is a slow process, lasting up to 2 to 4 weeks after malaria. This is in line with *in vitro* studies showing a slow recovery of the glycocalyx (39, 41, 42). Furthermore, elevated levels of angiopoetin-2 and inflammatory markers (43) have been shown to last for weeks after a malaria attack, hampering restoration (44).

The study had some limitations, since UM patients were significantly older than healthy controls and patients with NMF. Glycocalyx coverage may be influenced by age, although this has only been shown for young versus aged adults (45). Thus, the relatively small difference in age in this study is not expected to have an impact on interpretations. Gender has not been shown to result in any differences in glycocalyx coverage, and the difference in gender composition in the four groups is not expected to affect findings in the study. Furthermore, an increase in sample size, in particular for NMF patients, and more complete follow-up would have been desirable. Nevertheless, our data show robust differences between patient groups and to some extent support two recently published studies on glycocalyx loss in SM patients (23, 46). Plasma HRP2 was not measured, and thus a relationship between total parasite biomass and glycocalyx loss as well as level of hemorrhages could not be established.

In summary, IDF imaging has confirmed a previous study on microcirculatory changes in malaria. As a novel finding, it enabled assessment of microhemorrhages and visualization of sequestering parasites *in vivo*. Furthermore, it allowed us to demonstrate the loss of the endothelial glycocalyx in the buccal mucosa of human malaria patients. These vascular changes were mirrored by increased plasma levels of multiple glycocalyx components, including HA, which was positively correlated with the PBR. Shedding of the glycocalyx seemed related to endothelial activation and malaria severity, and the multitude of glycocalyx markers detected in plasma suggests that several proteases and glycosidases are activated during the disease. This should be investigated in further studies.

MATERIALS AND METHODS

Patients and enrollment. The study was a cross-sectional study designed to assess glycocalyx loss in pediatric malaria patients. Patients were admitted to the Magu district hospital, Mwanza region, Tanzania, during the high-transmission period (April to November 2017). Sample size was determined in a small pilot study ($n = 15$). In accordance with the hospital's routine admission procedures, the designated nurse/clinician screened the children for malaria, and before the child was enrolled into the study, informed

consent was obtained from the parent/guardian. The project was approved by the ethical committee of the National Institute for Medical Research Tanzania (NIMR/HQ/R.8c/Vol. II/715). All malaria patients enrolled were rapid diagnostic test (mRDT) positive (CareStart Malaria; Access Bio, NJ, USA) and had peripheral parasites counted in Giemsa-stained blood smears by a skilled microscopist. A lower cutoff of 1,000 infected erythrocytes/μl blood was set to avoid the inclusion of nonmalaria fever (NMF) patients in either of the groups of malaria patients. Patients were excluded from the study if they were less than 6 months old, had been admitted to a hospital less than a month before the current malaria attack, and if they had other complications (e.g., other infections) when admitted to the hospital with malaria. Malaria-negative individuals were enrolled from the same hospital from the Reproductive and Child Health Clinic; no neonates were enrolled in the study. Blood samples were collected, using sodium citrate as the anticoagulant, initially stored at −20°C, and then transferred to −80°C.

SM was defined as malaria with at least one of the following features (in accordance with WHO guidelines): seizures, lack of verbal and motor responses (Blantyre coma score [BCS] of less than or equal to 2), lactate level of >5 mM, hemoglobin (Hb) level of <5 g/dl (severe anemia), or hyperparasitemia (>10% parasitemia). Malaria patients without features associated with SM or SMA were termed uncomplicated malaria (UM) patients. Patients with NMF were RDT negative and were admitted to the children's ward with, e.g., diarrhea and urinary tract infections. Patient characteristics are found in Table 1, and a CONSORT diagram is supplied as Fig. S1 in the supplemental material. A breakdown of patients in the SM group is presented in Fig. 2.

Assessment of the microcirculation *in vivo*. Microcirculatory function was measured at the day of admission by incident dark-field (IDF) imaging (Cytocam, Braedius, The Netherlands). A handheld probe emits flashes (2 ms) of green light (525 nm) that is absorbed by hemoglobin in erythrocytes. Images are captured at a frame rate of 25 frames/s. The probe was placed on the buccal mucosa between the inferior lip and the teeth without causing local damage to the microvasculature. While the images were recorded, the quality of the movies was assessed by trained nurses and according to best practices (28), and at least three movies were recorded from each patient. Recordings were not included in the study if these criteria were not met (due to, e.g., shaken or compressed movies).

Analyses of IDF imaging. Cytocam software (version 1.7.12; Braedius) was used to crop and stabilize movie sequences. If fewer than three movies were considered adequate, the IDF data from that patient were excluded. For all analyses of IDF outputs, only a single value (mean/median) is reported per patient. The software automatically identifies blood vessels and can calculate total vessel density (TVD), perfused vessel density (PVD), proportion of perfused vessels (PPV), and average flow speed. We calculated the heterogeneity index as previously described (47). IDF imaging allowed a localized quantification of hemorrhages (stagnant erythrocytes). Stagnant erythrocytes were defined as immobile cells localized around vessels with flow. The field of view ($\sim$1.8 mm^2) was divided into 16 nonoverlapping rectangles, and the number of rectangles with hemorrhages was counted and divided by the total number of assessed rectangles; this fraction was reported as a percentage for each individual. Also, the proportions of individuals with hemorrhages were compared between the groups.

Furthermore, we developed software for studying erythrocyte movements. We developed a method by applying a pixel-wise filtering approach enabling us to calculate the width of a blood vessel and to analyze how erythrocytes move temporally. Blood vessel segments were cropped, and a minimum filter and a median filter were applied. Since erythrocytes absorb light and thus result in low pixel values, the minimum filter captures all positions (pixels) in which an erythrocyte has been present through all the analyzed frames and displays this in one output image. The median filter captures where erythrocytes most frequently have been present throughout the image sequence.

Edge detection (described by Canny [48]) was used to determine the boundary between the blood vessel and the surrounding tissue by using a standard deviation σ of 1.8. We applied a simplified version of Dijkstra's algorithm using pixel intensities as a cost measure for an automated selection of continuous edges of both sides of the blood vessels (49). This enabled us to determine the Euclidean widths along the length of the vessel. We did this after blurring images with a Gaussian filter (standard deviation σ = 5) and subsequently applying Dijkstra's algorithm to obtain a medial line of the vessel, followed by applying perpendicular lines to the medial line. The perpendicular lines were interpolated, and their corresponding intersections on the edges of the blood vessel were used to calculate the Euclidean distances for both the minimum and the median filter (Matlab, R2017a; Mathworks, MA, USA) (Fig. S4). This enabled in-depth analyses of multiple microvessel segments from multiple small movies from each patient. With these data, we calculated the perfused boundary region (PBR) as the Euclidian distance of the minimum filter minus the Euclidian distance of the median filter divided by 2. The median value of all the computed PBRs (>100/patient) was reported for each subject. The investigator was blinded to patient data when analyzing the movies.

Imaging of infected and uninfected erythrocytes *in vitro*. To assess how late-stage parasites appear in IDF imaging, *P. falciparum* (FCR3) was cultured in human type O erythrocytes as previously described (50). We produced a simple tissue phantom in 12-well plates, using 1% gelatin in RPMI 1640 (Biological Industries, Israel). Erythrocytes at 1% hematocrit diluted in 1% gelatin (diluted in RPMI 1640) were seeded and after gelation were imaged from above. We recorded IDF images of uninfected erythrocytes and late-stage-infected erythrocytes purified by magnetic assisted column separation as described previously (50). The images were assessed by line plots using Image J (version 1.52i) (51) and the Prewitt filter (Matlab). This filter was also applied to data obtained from the buccal cavity.

Plasma analyses. Plasma was analyzed by ELISA and multiplex-based Luminex (Magpix; R&D Systems, BioTechne, UK). The following plasma constituents were analyzed by ELISA: hyaluronic acid (HA; Echelon Biosciences, UT, USA), syndecan-4 (Quantikine; R&D Systems), and angiopoietin-1 (Quantikine;

R&D Systems). The following plasma constituents were analyzed by Luminex: syndecan-1, angiopoietin-2, TNF, E-selectin, thrombomodulin, CD44, and endothelin-1 (R&D Systems). Some healthy controls had endothelin-1 levels below the detection limit, which was set to the lowest value on the standard curve. All assays were performed according to the manufacturers' instructions, except that blocking was performed using 5% bovine serum albumin (BSA) for angiopoietin-1, as previously reported (52).

Also, 2 μl of plasma was blotted onto positively charged nitrocellulose (Amersham Hybond N^+; GE Healthcare, IL, USA). Standards for sulfated glycosaminoglycans (GAGs) (chondroitin sulfate A; Sigma-Aldrich, MI, USA), heparan sulfate (Sigma-Aldrich), and recombinant glypican-1 (Biolegend, CA, USA) were blotted. After drying, the membranes were blocked with skim milk (5% in Tris-buffered saline [TBS]; Sigma-Aldrich) for 1 h. Antibodies detecting human glypican-1 (R&D Systems) and heparan sulfate (clone 10E4; United States Biologicals, MA, USA) were diluted in blocking buffer and applied overnight at 4°C. Signals were detected by rabbit anti-goat antibody–horseradish peroxidase (HRP) (ThermoFisher, MA, USA), followed by goat anti-mouse IgM (Dylight680; Rockland Immunochemicals, Limerick, PA, USA). The signals were detected using an Odyssey Fc reader (LI-COR Biosciences, NE, USA). Examples of dot blots are shown in Fig. S6 in the supplemental material. Ultimately, the membranes were stained with Alcian blue as previously described (19, 20). Signal density was quantified using Image J (51). Markers were run for patients with satisfactory IDF imaging, and some markers (ELISA and dot blot assays) were also run for randomly selected individuals who had poor IDF movies (i.e., shaken, compressed). All analyses were performed in a blinded manner.

Statistical analyses. The sample size required to detect a 30% difference in glycocalyx loss was calculated from a small subset of patients enrolled in the first month of the study. Data were initially tested for normal distribution (Shapiro Wilks test) and equal variance (Bartlett's test). If data followed these criteria, parametric analyses were performed (analysis of variance [ANOVA] followed by Tukey's multiple-comparison tests). For some parameters, data followed these criteria after logarithmic conversion [$x' = \ln(x + 1)$]; otherwise, nonparametric analyses were performed (Kruskal-Wallis followed by Dunn's test). A chi-square test was performed to assess whether the proportion of subjects with hemorrhages was higher in SM patients than in healthy subjects. Logistic regression was applied to test for differences in perivascular hemorrhage densities. Correlation tests were performed with the nonparametric Spearman's rank correlation. Follow-up data were analyzed with Friedman's test, followed by a Dunn's test. All statistical analyses were performed using R for Windows (version 2.12.1) (53). Graphs were designed using GraphPad Prism (version 8.01; GraphPad, CA, USA).

SUPPLEMENTAL MATERIAL

Supplemental material for this article may be found at https://doi.org/10.1128/IAI.00679-19.

SUPPLEMENTAL FILE 1, PDF file, 4.7 MB.

SUPPLEMENTAL FILE 2, MPG file, 0.5 MB.

SUPPLEMENTAL FILE 3, MPG file, 3.1 MB.

ACKNOWLEDGMENTS

The contributions from all patients and parents as part of this study are inestimable. Without their consent, this work could not have been performed. Also, the support and help from the nurses at Magu district hospital, Lesha Constancia and Ghati Mwihechi, are greatly acknowledged, as well as the warm support and caring from Sospeter Ndegi.

This work was supported by a personal grant to C.H. by the Danish Research Council for Independent Research (grant number 6550-00554).

E.L. performed experiments, analyzed data, and contributed to the writing of the manuscript. L.E.H. developed software, performed experiments, analyzed data, and contributed to the writing of the manuscript. T.R. developed software, performed experiments, analyzed data, and contributed to the writing of the manuscript. C.W.W. supervised the project, researched the infrastructure, and contributed to the writing of the manuscript. A.M.E. collected data and contributed to the writing of the manuscript. A.M. supervised the project, researched the infrastructure, and contributed to the writing of the manuscript. V.M. supervised the project, researched the infrastructure, and contributed to the writing of the manuscript. J.L. supervised the project, researched the infrastructure, and contributed to the writing of the manuscript. T.G.T. supervised the project, researched the infrastructure, and contributed to the writing of the manuscript. J.A.L.K. supervised the project and contributed to the writing of the manuscript. R.P. developed software, analyzed the data, and contributed to the writing of the manuscript. C.H. conceived and planned experiments, attracted funding, analyzed the data, and wrote the manuscript with input from all coauthors.

REFERENCES

1. Storm J, Craig AG. 2014. Pathogenesis of cerebral malaria—inflammation and cytoadherence. Front Cell Infect Microbiol 4:100. https://doi.org/10.3389/fcimb.2014.00100.
2. Turner GD, Morrison H, Jones M, Davis TM, Looareesuwan S, Buley ID, Gatter KC, Newbold CI, Pukritayakamee S, Nagachinta B. 1994. An immunohistochemical study of the pathology of fatal malaria. Evidence for widespread endothelial activation and a potential role for intercellular adhesion molecule-1 in cerebral sequestration. Am J Pathol 145:1057–1069.
3. Higgins SJ, Purcell LA, Silver KL, Tran V, Crowley V, Hawkes M, Conroy AL, Opoka RO, Hay JG, Quaggin SE, Thurston G, Liles WC, Kain KC. 2016. Dysregulation of angiopoietin-1 plays a mechanistic role in the pathogenesis of cerebral malaria. Sci Transl Med 8:358ra128. https://doi.org/10.1126/scitranslmed.aaf6812.
4. Conroy AL, Lafferty EI, Lovegrove FE, Krudsood S, Tangpukdee N, Liles WC, Kain KC. 2009. Whole blood angiopoietin-1 and -2 levels discriminate cerebral and severe (non-cerebral) malaria from uncomplicated malaria. Malar J 8:295. https://doi.org/10.1186/1475-2875-8-295.
5. Hempel C, Pasini EM, Kurtzhals JA. 2016. Endothelial glycocalyx: shedding light on malaria pathogenesis. Trends Mol Med 22:453–457. https://doi.org/10.1016/j.molmed.2016.04.004.
6. Bridges DJ, Bunn J, van Mourik JA, Grau G, Preston RJS, Molyneux M, Combes V, O'Donnell JS, de Laat B, Craig A. 2010. Rapid activation of endothelial cells enables Plasmodium falciparum adhesion to platelet-decorated von Willebrand factor strings. Blood 115:1472–1474. https://doi.org/10.1182/blood-2009-07-235150.
7. Turner L, Lavstsen T, Berger SS, Wang CW, Petersen JE, Avril M, Brazier AJ, Freeth J, Jespersen JS, Nielsen MA, Magistrado P, Lusingu J, Smith JD, Higgins MK, Theander TG. 2013. Severe malaria is associated with parasite binding to endothelial protein C receptor. Nature 498:502–505. https://doi.org/10.1038/nature12216.
8. Lennartz F, Adams Y, Bengtsson A, Olsen RW, Turner L, Ndam NT, Ecklu-Mensah G, Moussiliou A, Ofori MF, Gamain B, Lusingu JP, Petersen JE, Wang CW, Nunes-Silva S, Jespersen JS, Lau CK, Theander TG, Lavstsen T, Hviid L, Higgins MK, Jensen AT. 2017. Structure-guided identification of a family of dual receptor-binding PfEMP1 that is associated with cerebral malaria. Cell Host Microbe 21:403–414. https://doi.org/10.1016/j.chom.2017.02.009.
9. Wassmer SC, Moxon CA, Taylor T, Grau GE, Molyneux ME, Craig AG. 2011. Vascular endothelial cells cultured from patients with cerebral or uncomplicated malaria exhibit differential reactivity to TNF. Cell Microbiol 13:198–209. https://doi.org/10.1111/j.1462-5822.2010.01528.x.
10. Lovegrove FE, Tangpukdee N, Opoka RO, Lafferty EI, Rajwans N, Hawkes M, Krudsood S, Looareesuwan S, John CC, Liles WC, Kain KC. 2009. Serum angiopoietin-1 and -2 levels discriminate cerebral malaria from uncomplicated malaria and predict clinical outcome in African children. PLoS One 4:e4912. https://doi.org/10.1371/journal.pone.0004912.
11. Reitsma S, Slaaf DW, Vink H, van Zandvoort MA, Oude Egbrink MG. 2007. The endothelial glycocalyx: composition, functions, and visualization. Pflugers Arch 454:345–359. https://doi.org/10.1007/s00424-007-0212-8.
12. Marki A, Esko JD, Pries AR, Ley K. 2015. Role of the endothelial surface layer in neutrophil recruitment. J Leukoc Biol 98:503–515. https://doi.org/10.1189/jlb.3MR0115-011R.
13. Florian JA, Kosky JR, Ainslie K, Pang Z, Dull RO, Tarbell JM. 2003. Heparan sulfate proteoglycan is a mechanosensor on endothelial cells. Circ Res 93:e136–e142. https://doi.org/10.1161/01.RES.0000101744.47866.D5.
14. Betteridge K, Arkill K, Neal C, Harper S, Foster B, Satchell S, Bates D, Salmon A. 2017. Sialic acids regulate microvessel permeability, revealed by novel in vivo studies of endothelial glycocalyx structure and function. J Physiol 595:5015–5035. https://doi.org/10.1113/JP274167.
15. Nussbaum C, Cavalcanti Fernandes Heringa A, Mormanova Z, Puchwein-Schwepcke AF, Bechtold-Dalla Pozza S, Genzel-Boroviczény O. 2014. Early microvascular changes with loss of the glycocalyx in children with type 1 diabetes. J Pediatr 164:584–589.e1. https://doi.org/10.1016/j.jpeds.2013.11.016.
16. Nelson A, Berkestedt I, Schmidtchen A, Ljunggren L, Bodelsson M. 2008. Increased levels of glycosaminoglycans during septic shock: relation to mortality and the antibacterial actions of plasma. Shock 30:623–627. https://doi.org/10.1097/SHK.0b013e3181777da3.
17. Ozturk B, Kuscu F, Tutuncu E, Sencan I, Gurbuz Y, Tuzun H. 2010. Evaluation of the association of serum levels of hyaluronic acid, sICAM-1, sVCAM-1, and VEGF-A with mortality and prognosis in patients with Crimean-Congo hemorrhagic fever. J Clin Virol 47:115–119. https://doi.org/10.1016/j.jcv.2009.10.015.
18. Suwarto S, Sasmono RT, Sinto R, Ibrahim E, Suryamin M. 2017. Association of endothelial glycocalyx and tight and adherens junctions with severity of plasma leakage in dengue infection. J Infect Dis 215:992–999. https://doi.org/10.1093/infdis/jix041.
19. Hempel C, Hyttel P, Kurtzhals JA. 2014. Endothelial glycocalyx on brain endothelial cells is lost in experimental cerebral malaria. J Cereb Blood Flow Metab 34:1107–1110. https://doi.org/10.1038/jcbfm.2014.79.
20. Hempel C, Sporring J, Kurtzhals J. 2018. Experimental cerebral malaria is associated with profound loss of both glycan and protein components of the endothelial glycocalyx. FASEB J 33:2058–2071. https://doi.org/10.1096/fj.201800657R:fj201800657R.
21. Craig AG, Grau GE, Janse C, Kazura JW, Milner D, Barnwell JW, Turner G, Langhorne J, Participants of the Hinxton Retreat Meeting on Animal Models for Research on Severe Malaria. 2012. The role of animal models for research on severe malaria. PLoS Pathog 8:e1002401. https://doi.org/10.1371/journal.ppat.1002401.
22. Muanza K, Traore B, Gay F, Krudsood S, Danis M, Looareesuwan S. 1999. Circulating receptors implicated in the cyto-adherence occurring in severe Plasmodium falciparum malaria in Thailand. Ann Trop Med Parasitol 93:449–455. https://doi.org/10.1080/00034989958186.
23. Yeo TW, Weinberg JB, Lampah DA, Kenangalem E, Bush P, Chen Y, Price RN, Young S, Zhang HY, Millington D, Granger DL, Anstey NM. 2019. Glycocalyx breakdown is associated with severe disease and fatal outcome in Plasmodium falciparum malaria. Clin Infect Dis 69:1712–1720. https://doi.org/10.1093/cid/ciz038.
24. Graham SM, Chen J, Chung DW, Barker KR, Conroy AL, Hawkes MT, Namasopo S, Kain KC, Lopez JA, Liles WC. 2016. Endothelial activation, haemostasis and thrombosis biomarkers in Ugandan children with severe malaria participating in a clinical trial. Malar J 15:56. https://doi.org/10.1186/s12936-016-1106-z.
25. Lee DH, Dane MJ, van den Berg BM, Boels MG, van Teeffelen JW, de Mutsert R, den Heijer M, Rosendaal FR, van der Vlag J, van Zonneveld AJ, Vink H, Rabelink TJ, for the NEO Study Group. 2014. Deeper penetration of erythrocytes into the endothelial glycocalyx is associated with impaired microvascular perfusion. PLoS One 9:e96477. https://doi.org/10.1371/journal.pone.0096477.
26. Milner DA, Jr, Whitten RO, Kamiza S, Carr R, Liomba G, Dzamalala C, Seydel KB, Molyneux ME, Taylor TE. 2014. The systemic pathology of cerebral malaria in African children. Front Cell Infect Microbiol 4:104. https://doi.org/10.3389/fcimb.2014.00104.
27. Dondorp AM, Ince C, Charunwatthana P, Hanson J, van Kuijen A, Faiz MA, Rahman MR, Hasan M, Bin Yunus E, Ghose A, Ruangveerayut R, Limmathurotsakul D, Mathura K, White NJ, Day NP. 2008. Direct in vivo assessment of microcirculatory dysfunction in severe falciparum malaria. J Infect Dis 197:79–84. https://doi.org/10.1086/523762.
28. De Backer D, Hollenberg S, Boerma C, Goedhart P, Buchele G, Ospina-Tascon G, Dobbe I, Ince C. 2007. How to evaluate the microcirculation: report of a round table conference. Crit Care 11:R101. https://doi.org/10.1186/cc6118.
29. Ince C. 2015. Hemodynamic coherence and the rationale for monitoring the microcirculation. Crit Care 19(Suppl 3):S8. https://doi.org/10.1186/cc14726.
30. White NJ. 2018. Anaemia and malaria. Malar J 17:371. https://doi.org/10.1186/s12936-018-2509-9.
31. Greiner J, Dorovini-Zis K, Taylor TE, Molyneux ME, Beare NA, Kamiza S, White VA. 2015. Correlation of hemorrhage, axonal damage, and blood-tissue barrier disruption in brain and retina of Malawian children with fatal cerebral malaria. Front Cell Infect Microbiol 5:18. https://doi.org/10.3389/fcimb.2015.00018.
32. Thurston G, Suri C, Smith K, McClain J, Sato TN, Yancopoulos GD, McDonald DM. 1999. Leakage-resistant blood vessels in mice transgenically overexpressing angiopoietin-1. Science 286:2511–2514. https://doi.org/10.1126/science.286.5449.2511.
33. Cai C, Carey KA, Nedosekin DA, Menyaev YA, Sarimollaoglu M, Galanzha EI, Stumhofer JS, Zharov VP. 2016. In vivo photoacoustic flow cytometry for early malaria diagnosis. Cytometry A 89:531–542. https://doi.org/10.1002/cyto.a.22854.
34. Olliaro P, Lombardi L, Frigerio S, Basilico N, Taramelli D, Monti D. 2000.

Phagocytosis of hemozoin (native and synthetic malaria pigment), and Plasmodium falciparum intraerythrocyte-stage parasites by human and mouse phagocytes. Ultrastruct Pathol 24:9–13. https://doi.org/10.1080/019131200281264.
35. Schwarzer E, Bellomo G, Giribaldi G, Ulliers D, Arese P. 2001. Phagocytosis of malarial pigment haemozoin by human monocytes: a confocal microscopy study. Parasitology 123:125–131. https://doi.org/10.1017/s0031182001008216.
36. Stevens AP, Hlady V, Dull RO. 2007. Fluorescence correlation spectroscopy can probe albumin dynamics inside lung endothelial glycocalyx. Am J Physiol Lung Cell Mol Physiol 293:L328–L335. https://doi.org/10.1152/ajplung.00390.2006.
37. Squire JM, Chew M, Nneji G, Neal C, Barry J, Michel C. 2001. Quasi-periodic substructure in the microvessel endothelial glycocalyx: a possible explanation for molecular filtering? J Struct Biol 136:239–255. https://doi.org/10.1006/jsbi.2002.4441.
38. Chappell D, Dorfler N, Jacob M, Rehm M, Welsch U, Conzen P, Becker BF. 2010. Glycocalyx protection reduces leukocyte adhesion after ischemia/reperfusion. Shock 34:133–139. https://doi.org/10.1097/SHK.0b013e3181cdc363.
39. Hempel C, Wang CW, Kurtzhals JAL, Staalso T. 2017. Binding of Plasmodium falciparum to CD36 can be shielded by the glycocalyx. Malar J 16:193. https://doi.org/10.1186/s12936-017-1844-6.
40. Hippensteel JA, Anderson BJ, Orfila JE, McMurtry SA, Dietz RM, Su G, Ford JA, Oshima K, Yang Y, Zhang F, Han X, Yu Y, Liu J, Linhardt RJ, Meyer NJ, Herson PS, Schmidt EP. 2019. Circulating heparan sulfate fragments mediate septic cognitive dysfunction. J Clin Invest 129:1779–1784. https://doi.org/10.1172/JCI124485.
41. Bai K, Wang W. 2012. Spatio-temporal development of the endothelial glycocalyx layer and its mechanical property in vitro. J R Soc Interface 9:2290–2298. https://doi.org/10.1098/rsif.2011.0901.
42. Potter DR, Jiang J, Damiano ER. 2009. The recovery time course of the endothelial cell glycocalyx in vivo and its implications in vitro. Circ Res 104:1318–1325. https://doi.org/10.1161/CIRCRESAHA.108.191585.
43. Moxon CA, Chisala NV, Wassmer SC, Taylor TE, Seydel KB, Molyneux ME, Faragher B, Kennedy N, Toh CH, Craig AG, Heyderman RS. 2014. Persistent endothelial activation and inflammation after Plasmodium falciparum infection in Malawian children. J Infect Dis 209:610–615. https://doi.org/10.1093/infdis/jit419.
44. Lukasz A, Hillgruber C, Oberleithner H, Kusche-Vihrog K, Pavenstädt H, Rovas A, Hesse B, Goerge T, Kümpers P. 2017. Endothelial glycocalyx breakdown is mediated by angiopoietin-2. Cardiovasc Res 113:671–680. https://doi.org/10.1093/cvr/cvx023.
45. Machin DR, Bloom SI, Campbell RA, Phuong TTT, Gates PE, Lesniewski LA, Rondina MT, Donato AJ. 2018. Advanced age results in a diminished endothelial glycocalyx. Am J Physiol Heart Circ Physiol 315:H531–H539. https://doi.org/10.1152/ajpheart.00104.2018.
46. Yeo TW, Bush PA, Chen Y, Young SP, Zhang H, Millington DS, Granger DL, Mwaikambo ED, Anstey NM, Weinberg JB. 2019. Glycocalyx breakdown is increased in African children with cerebral and uncomplicated falciparum malaria. FASEB J 33:14185–14193. https://doi.org/10.1096/fj.201901048RR:fj201901048RR.
47. De Backer D, Orbegozo Cortes D, Donadello K, Vincent JL. 2014. Pathophysiology of microcirculatory dysfunction and the pathogenesis of septic shock. Virulence 5:73–79. https://doi.org/10.4161/viru.26482.
48. Canny J. 1986. A computational approach to edge detection. IEEE Trans Pattern Anal Mach Intell 8:679–698.
49. Paulsen RRM, Moeslund TB. 2016. Introduction to medical image analysis. DTU Compute, Kongens Lyngby, Denmark.
50. Hempel C, Kohnke H, Maretty L, Jensen PO, Staalso T, Kurtzhals JA. 2014. Plasmodium falciparum avoids change in erythrocytic surface expression of phagocytosis markers during inhibition of nitric oxide synthase activity. Mol Biochem Parasitol 198:29–36. https://doi.org/10.1016/j.molbiopara.2014.11.003.
51. Schindelin J, Arganda-Carreras I, Frise E, Kaynig V, Longair M, Pietzsch T, Preibisch S, Rueden C, Saalfeld S, Schmid B, Tinevez JY, White DJ, Hartenstein V, Eliceiri K, Tomancak P, Cardona A. 2012. Fiji: an open-source platform for biological-image analysis. Nat Methods 9:676–682. https://doi.org/10.1038/nmeth.2019.
52. Hempel C, Hoyer N, Kildemoes A, Jendresen CB, Kurtzhals JA. 2014. Systemic and cerebral vascular endothelial growth factor levels increase in murine cerebral malaria along with increased calpain and caspase activity and can be reduced by erythropoietin treatment. Front Immunol 5:291. https://doi.org/10.3389/fimmu.2014.00291.
53. R Core Team. 2008. R: a language and environment for statistical computing. R Foundation for Statistical Computing, Vienna, Austria.